

Supplemental Materials

Abbreviations: *HC*, healthy controls; *SZ*, schizophrenia subjects; *ESZ*, early illness schizophrenia subjects; *CSZ*, chronic illness schizophrenia subjects.

Additional task description details

The display screen consisted of three reels that populated with fruit symbols with an interstimulus interval of 1 second. There were 12 possible fruit symbols that were equally distributed across conditions (clip art from <https://openclipart.org>); thus, no individual symbol carried predictive information about reward outcomes. Subjects self-initiated each trial via a button press that triggered the simulated coin drop and slot machine lever pull, after which reels 1-3 (i.e., R1, R2, R3) populated automatically from left to right. After R3 populated, a 10Hz visual checkerboard flickered for 1000 ms followed by text indicating the outcome (i.e., “WIN \$1.25” or “LOSE”). Sound effects (e.g., coin dropping audio) and visualizations (e.g., coin insertion, lever pull) enhanced the task’s ecological validity.

The *reward anticipation* phase spanned the population of R1 and R2 and the anticipation of R3. The *reward evaluation phase* began when R3 populated. Total trial time was 6115 ms.

Additional EEG data denoising procedures

Electro-oculogram (EOG) data were recorded from electrodes placed above and below the left eye and at the outer canthi of both eyes to capture vertical (VEOG) and horizontal (HEOG) eye movements. The Fully Automated Statistical Thresholding for EEG artifact Rejection (FASTER) MATLAB-based toolbox was used to clean the raw EEG epochs (Nolan et al., 2010). Like our previous reports (Hamilton et al., 2019), the FASTER processing approach was modified here between steps 2 and 3 to include canonical correlation analysis (CCA, see below for more detail). The FASTER method employs multiple descriptive measures to search for statistical outliers (± 3 SD from mean). This process included 4 steps: (1) outlier channels were identified and replaced with interpolated values in continuous data, (2) outlier epochs were removed from participants’ single trial set, (3) spatial independent components analysis was applied to remaining trials, outlier components were identified using the ADJUST procedure (Mognon et al., 2011), and data were back-projected without these components, and (4) within an epoch, outlier channels were interpolated. Epochs were time-locked to the onset of stimulus and baseline corrected (-100 to 0 ms).

Canonical correlation analysis (CCA) was used as a blind source separation technique to remove broadband or electromyographic noise from single trial electroencephalographic (EEG) data, generating de-noised EEG epochs. Our approach is similar to the CCA method described by others (De Clercq et al., 2006; Riès et al., 2013), and previously applied to other studies, with some important differences. The method is based on the concepts that true EEG data tend to show high auto-correlation and exhibit power-law scaling (i.e., power is proportional to $1/\text{frequency}$), but that high

frequency random noise in EEG (e.g., muscle artifact, electromyographic (EMG)) tends to show low auto-correlation and violates power-law scaling (i.e., inappropriately high power at higher frequencies relative to low frequencies). The CCA de-noising procedure is performed separately for each subject on the single trial EEG epoch data. For a 3 second epoch, the $(S \times X)$ matrix containing the time series of $S = 3072$ EEG samples ($s_1, s_2, s_3 \dots s_{3072}$) at each of $X = 64$ scalp electrodes ($x_1, x_2, x_3 \dots x_{64}$) is subjected to a CCA with the $(S \times Y)$ matrix containing the $s + 1$ time-lagged series of 3072 EEG samples ($s_2, s_3, s_4 \dots s_{3072}, s_{3073}$, where $s_{3073} = 0$) at each of the same 64 electrodes ($y_1, y_2, y_3 \dots y_{64}$). This is the multivariate equivalent of auto-regressive time series correlation. Since both the X and Y vectors each contain 64 electrodes, a total of 64 canonical correlations can be extracted. Each canonical correlation coefficient expresses the correlation of a time series of values representing the weighted sums of the X electrodes with a $s + 1$ time series of values representing the weighted sums of the Y electrodes, with weights chosen to yield the largest canonical correlation that accounts for variance independent of the variance accounted for by all previously extracted canonical correlations. Thus, each canonical correlation coefficient has an associated time series of values that constitutes the canonical variate, X (i.e., each time point has a value that is a linear function of the canonical weights and raw data associated with the 64 electrodes), as well as a similar canonical variate, Y . The current CCA de-noising method only makes use of the set of 64 canonical X variates, one for each of the 64 extracted canonical correlations. When the time series represented by a canonical variate is subjected to a fast Fourier transformation (FFT), the resulting power spectrum can be evaluated to determine whether the canonical variate conforms to the power-law expected from EEG data, in which case it should be retained, or whether it violates the power law as would be expected for high-frequency noise (e.g., EMG contamination), in which case it should be excluded. With this approach, the retained canonical variates are those showing the strongest canonical correlations, whereas the rejected canonical variates are those showing the weakest canonical correlations. The specific criterion used to make these retain/reject decisions is where our CCA denoising approach differs from previously published approaches from other labs (e.g., Riès et al., 2013), but is consistent with our other reports (Hamilton et al., 2019; Kort et al., 2017).

ERP age-matched HC subgroups

As shown in Table 1, there were significant differences in age between the three groups. And as described in the main text, we used an age-adjustment procedure to account for these inherent differences; however, to be certain that our between-group ERP effects were not driven by these demographic differences, we performed follow-up analyses using age-matched HC subgroups. HC subjects were divided into two age-matched subgroups using a median split: i) younger HC ($n = 27$) = 23.15 ± 2.07 years vs. ESZ ($n = 26$) 24.47 ± 4.01 years, and ii) older HC ($n = 27$) = 44.28 ± 13.69 years vs. CSZ ($n = 28$) = 44.05 ± 14.73 years. There were no significant differences in age or gender (all $p > .10$) in either matched group set.

ERP grand averages

As described previously, there was a significant negative relationship between age and RewP in HC (Fryer et al., 2020). We therefore present the grand averages of the RewP difference waveforms in Figure 2, with HC separated into younger and older subgroups (determined via median split as described above). Figure S2 shows the frontal-central scalp distribution of the RewP difference waves, again with HC separated into younger and older subgroups. We note that the RewP difference score was significantly larger when measured at R3 versus R2 for HC, ESZ, and CSZ (all $p < .01$), consistent with complete reward feedback delivery occurring at R3.

ERP age-matched subgroup re-analysis

When using age-matched HC subgroups and raw SPN scores, the Group x Condition interactions remained non-significant (younger HC vs. ESZ: $F_{1,51} = 0.14$, $p = .71$; older HC vs. CSZ: $F_{1,52} = 0.04$, $p = .83$). However, CSZ had lower SPN amplitudes, overall, relative to older HC; $F_{1,52} = 6.15$, $p = .02$, indicating reduced anticipation among CSZ when expecting reward or non-reward feedback. (One CSZ subject was removed who had an SPN value ± 3 SD from the mean.)

There was no effect of Group when comparing ESZ and CSZ to age-matched HC subgroups using the unadjusted RewP data (younger HC vs. ESZ: $t_{51} = 0.73$, $p = .47$; older HC vs. CSZ: $t_{53} = -0.16$, $p = .87$).

Finally, we observed the same pattern of LPP group differences, with ESZ showing a heightened near miss response relative to younger HC ($F_{1,50} = 8.71$, $p = .005$; Figure S3), versus no difference between CSZ and older HC ($F_{1,52} = 0.00$, $p = .97$). (One ESZ and one CSZ subject were removed who had LPP values ± 3 SD from the mean.)

BrainAGE Model

Results from the HC BrainAGE model are presented in Table S2. We observed a significant negative age-relationship with RewP, indicating reduced win-related reward responsiveness with age. We also found a positive relationship between age and the LPP average, which could mean that the salience of non-specific motivational factors (wins and losses) increases with age. Further, the SPN difference score's (possible wins AA – total misses AB) contribution to the model was marginally significant. Taken together, the HC age regression model used to derive estimates of BrainAGE indicated that with increasing age, HC have reduced early reward evaluation response (RewP), elevated attention to reward outcomes regardless of valence (average LPP), and marginally reduced reward anticipation signaling (SPN).

Table S1. Correlations between original and age-adjusted ERP amplitudes

HC	<i>r</i>	<i>R</i> ²
SPN (AA)	.99	.97
SPN (AB)	.99	.99
RewP (difference score)	.89	.79
LPP (AAA – ABC)	1.00	1.00
LPP (AAB – ABC)	1.00	1.00

SZ	<i>r</i>	
SPN (AA)	1.00	.99
SPN (AB)	1.00	.99
RewP (difference score)	.88	.77
LPP (AAA – ABC)	1.00	1.00
LPP (AAB – ABC)	1.00	1.00

Table S2. Age-adjusted LPP Group x Condition follow-up tests

	t-ratio	p-value	p-adj
Contrast			
<i>Win Condition (AAA – ABC)</i>			
HC wins vs. ESZ wins	0.77	.44	.86
HC wins vs. CSZ wins	0.41	.69	.86
ESZ wins vs. CSZ wins	-.31	.76	.86
<i>Near Miss Condition (AAB – ABC)</i>			
HC near misses vs. ESZ near misses	-1.37	.17	.47
HC near misses vs. CSZ near misses	0.34	.73	.86
ESZ near misses vs. CSZ near misses	1.46	.15	.47
<i>Win vs. Near Miss (AAA – ABC vs. AAB – ABC)</i>			
ESZ wins vs. ESZ near misses	-3.18	.002	.02
CSZ wins vs. CSZ near misses	-.09	.93	.93

Abbreviations: *p-adj*, FDR-adjusted p-values; *HC*, healthy controls; *ESZ*, early illness schizophrenia subjects; *CSZ*, chronic illness schizophrenia subjects.

Table S3. HC Brain Age Model

	β (SE)	t-stat	p-value	VIF
SPN (AA – AB)	.24 (.13)	1.79	.08	1.34
RewP (AAA – AAA)	-.53 (.12)	-4.43	<.001	1.06
LPP (AAA + AAB)/2	.41 (.14)	3.02	.004	1.38
LPP (AAA – AAB)	-.03 (.12)	-0.26	.79	1.03

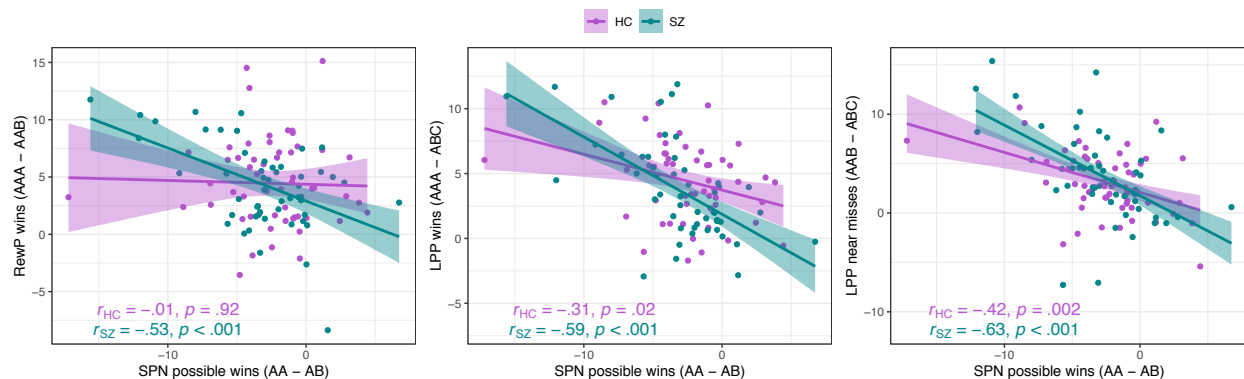
$F_{4,49} = 6.21, p < .001, \text{Adjusted } R^2 = .28$

Abbreviations: *VIF*, variance inflation factor; *SPN*, stimulus preceding negativity; *RewP*, reward positivity; *LPP*, late positive potential; *AA*, possible wins; *AB* total misses; *AAA*, wins; *AAB*, near misses.

Mean absolute error = 9.37; Root mean square error = 11.63

Correlation between chronological and predicted ages for HC: $r_{52} = .58, p < .001$

Figure S1. Relationships among reward ERP components

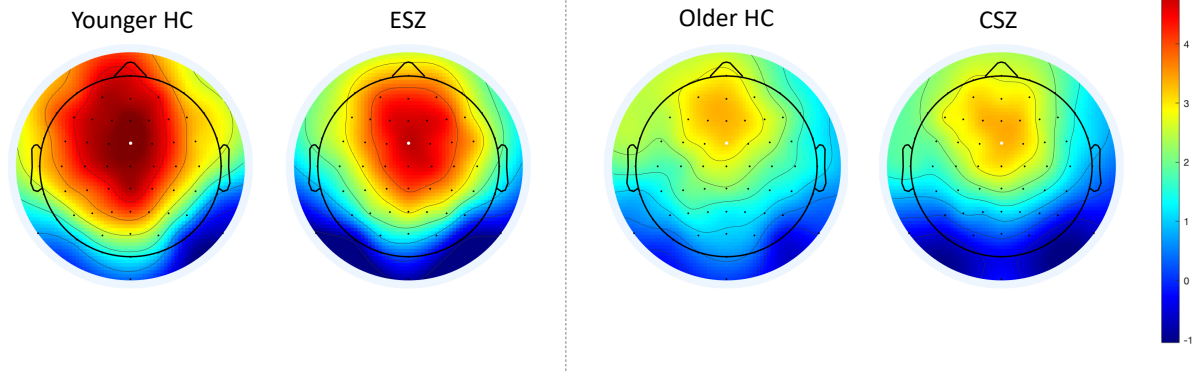


(A) Correspondence between stimulus-preceding negativity (SPN) reward anticipation (AA - AB) with reward positivity (RewP) difference scores (AAA - AAB) across groups (HC, healthy controls; SZ, schizophrenia subjects). **(B)** Correspondence between SPN reward anticipation with late-positive potential (LPP) win scores (AAA - ABC) across groups. **(C)** Correspondence between SPN reward anticipation with LPP near miss scores (AAB - ABC) across groups. For all analyses, we removed two SZ subjects with an average SPN value on AB trials ± 3 SD from the mean; for the LPP win analyses, we removed three SZ subjects with an average value ± 3 SD from the mean; and for the LPP near miss analyses, we removed one SZ subject with a value ± 3 SD from the mean.

Figure S2. RewP difference score topographical maps

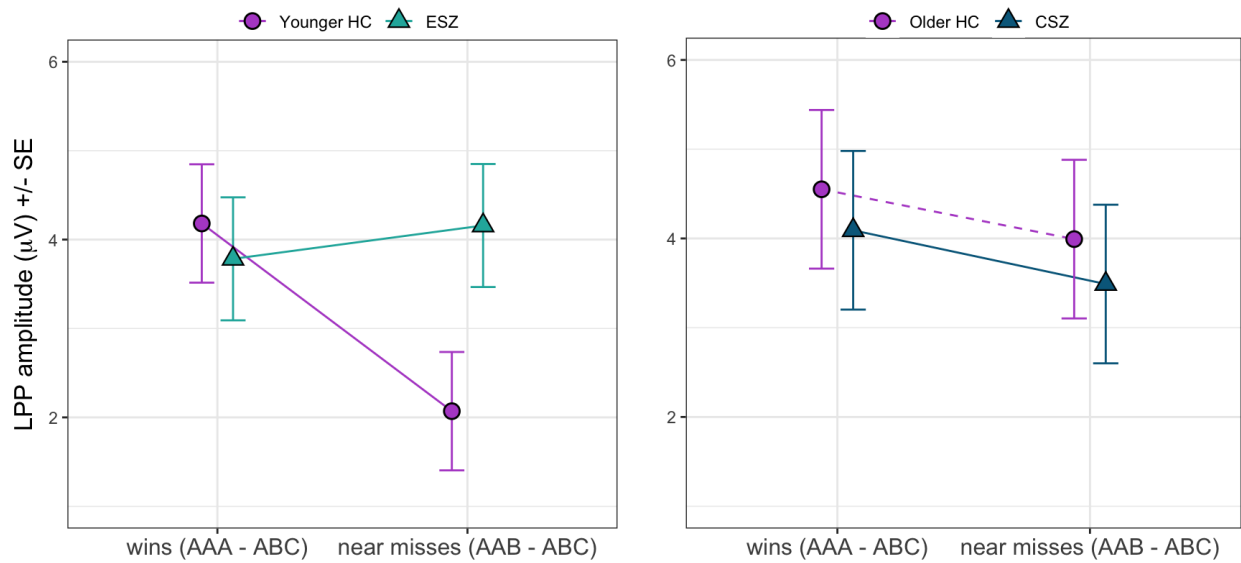
FCz

Reel 3: wins (AAA) – near misses (AAB)



Topographical maps of condition difference waves at Reel 3 for all groups, wins (AAA) – near misses (AAB).

Figure S3. LPP group differences using age-matched HC subgroups



Early illness schizophrenia subjects (ESZ) showed a heightened near miss response relative to the younger healthy control (HC) subgroup when using unadjusted late positive potential (LPP) amplitudes (*left*). No Group x Condition interaction emerged when comparing chronic schizophrenia subjects (CSZ) with older HC subjects (*right*).

References

- De Clercq, W., Vergult, A., Vanrumste, B., Van Paesschen, W., & Van Huffel, S. (2006). Canonical correlation analysis applied to remove muscle artifacts from the electroencephalogram. *IEEE Transactions on Biomedical Engineering*, *53*(12), 2583–2587.
- Fryer, S. L., Roach, B. J., Holroyd, C. B., Paulus, M. P., Sargent, K., Boos, A., Mathalon, D. H., & Ford, J. M. (2020). Electrophysiological investigation of reward anticipation and outcome evaluation during slot machine play. *BioRxiv*.
- Hamilton, H. K., Roach, B. J., Bachman, P. M., Belger, A., Carrion, R. E., Duncan, E., Johannesen, J. K., Light, G. A., Niznikiewicz, M. A., Addington, J., Bearden, C. E., Cadenhead, K. S., Cornblatt, B. A., McGlashan, T. H., Perkins, D. O., Seidman, L. J., Tsuang, M. T., Walker, E. F., Woods, S. W., ... Mathalon, D. H. (2019). Association Between P300 Responses to Auditory Oddball Stimuli and Clinical Outcomes in the Psychosis Risk Syndrome. *JAMA Psychiatry*, *76*(11), 1187–1197.
- Kort, N. S., Ford, J. M., Roach, B. J., Gunduz-Bruce, H., Krystal, J. H., Jaeger, J., Reinhart, R. M. G., & Mathalon, D. H. (2017). Role of N-Methyl-D-Aspartate Receptors in Action-Based Predictive Coding Deficits in Schizophrenia. *Biological Psychiatry*, *81*(6), 514–524.
- Mognon, A., Jovicich, J., Bruzzone, L., & Buiatti, M. (2011). ADJUST: An automatic EEG artifact detector based on the joint use of spatial and temporal features. *Psychophysiology*, *48*(2), 229–240.
- Nolan, H., Whelan, R., & Reilly, R. B. (2010). FASTER: Fully Automated Statistical Thresholding for EEG artifact Rejection. *Journal of Neuroscience Methods*, *192*(1), 152–162.
- Riès, S., Janssen, N., Burle, B., & Alario, F. X. (2013). Response-Locked Brain Dynamics of Word Production. *PLoS ONE*, *8*(3), e58197.